A&A 435, 459–463 (2005)
DOI: 10.1051/0004-6361:20041394

Astronomy & Astrophysics

HI observations of edge-on spiral galaxies⋆,⋆⋆

W. K. Huchtmeier[1], I. D. Karachentsev[2], V. E. Karachentseva[3], Yu. N. Kudrya[3], and S. N. Mitronova[2,4]

[1] Max-Planck-Institut für Radioastronomie, Auf dem Hügel 69, 53121 Bonn, Germany
e-mail: huchtmeier@mpifr-bonn.mpg.de
[2] Special Astrophysical Observatory, Russian Academy of Sciences, N.Arkhyz, KChR 369167, Russia
[3] Astronomical Observatory of Kiev University, Kiev, Ukraine
[4] Isaac Newton Institute of Chile, SAO Branch, Russia

Received 3 June 2004 / Accepted 7 January 2005

Abstract. Neutral hydrogen observations with the 100-m Effelsberg radio telescope are presented for 268 spiral galaxies from the Revised Flat Galaxy Catalog. Fluxes, radial velocities and line widths are given for 121 detected galaxies, as well as search parameters for 147 undetected objects. Most of the detected galaxies are late type (Sbc – Sdm) spirals with a mean M_{25}/L_B ratio of 2.5 in solar units. (M_{25} is the total mass within the $25^{\rm m}/\Box''$ isophote) and a mean hydrogen mass fraction $M_{\rm HI}/M_{25} = 0.13$. Correlations between global parameters are discussed briefly. A comparison with a sample of nearby galaxies (within 10 Mpc) demonstrates the validity of the same linear relation between the optical luminosity (L_B) and the linear diameter (A_{25}) down to the smallest galaxies.

Key words. galaxies: fundamental parameters – galaxies: spiral – galaxies: general

1. Introduction

A thorough inspection of the blue and red images of the sky surveys POSS-I and ESO/SERC resulted in the construction of a catalog of flat edge-on spiral galaxies. The following selection criteria were applied: blue angular diameters greater than $a_{\rm lim} = 0'.6$ and apparent blue axial ratios $a/b > 7$. The revised and complemented version of the catalog, RFGC (Revised Flat Galaxy Catalog, Karachentsev et al. 1999a) involves 4236 flat galaxies. The catalog has been prepared for a study of the large-scale streaming of galaxies (Karachentsev 1989; Karachentsev et al. 2000a).

The publication of the complete and homogeneous Two Micron All-Sky Survey (2MASS, Skrutskie et al. 1997) opens up new opportunities for a cosmic flow study via the NIR Tully-Fisher relation (Kudrya et al. 2003). The majority (71%) of the RFGC galaxies have quite accurate J, H, K photometry in the 2MASS catalogue, but only 25% of them have accurate data on their radial velocities as well as HI line widths. HI observations of flat galaxies were carried out by Giovanelli et al. (1997) using the Arecibo 305-m radio telescope. Later, Makarov et al. (2001) derived rotation curves for ∼300 RFGC galaxies based on spectroscopy with the 6-m SAO telescope. A compilation of all accessible data of the heliocentric radial velocity $V_{\rm h}$ and their half power HI line width W_{50} for RFGC galaxies was published by Karachentsev et al. (2000b). All the above-mentioned data, including the HI data from this paper, were used in our recent publication on a cosmic flow study of RFGC galaxies (Kudrya et al. 2003).

In this paper we present results of new HI observations for RFGC galaxies made with the Effelsberg 100-m radio telescope and briefly discuss some statistical properties of the sample. We compare the main properties of our sample with those of the FGC Arecibo sample of Karachentsev et al. (1999b) and a sample of the local volume galaxies (Karachentsev et al. 2004).

2. Observations

New HI observations of RFGC galaxies with the 100-m radio telescope at Effelsberg were initiated in order to increase the number of galaxies and the sky coverage of the sample for an improved determination of the large-scale streaming of galaxies. The HI line observations of flat galaxies were performed using the Effelsberg 100-m radio telescope during several sessions between October 2001 and April 2002. The target list was obtained by selecting the RFGC galaxies which are located in the declination range north of −31°, accessible for the Effelsberg telescope.

For galaxies having no data on $V_{\rm h}$ or W_{50} we calculated their rough predicted radial velocities ($V_{\rm pred}$) using two empirical relations between $V_{\rm h}$ and $J_{\rm 20fe}$ (infra-red J magnitude from 2MASS survey, see Kudrya et al. 2003), and between $V_{\rm h}$ and $(B - J_{\rm 20fe})$ for those RFGC galaxies where these data

⋆ Figure 1 is only available in electronic form at http://www.edpsciences.org

⋆⋆ Tables 1 and 2 are only available in electronic form at the CDS via anonymous ftp to cdsarc.u-strasbg.fr (130.79.128.5) or via http://cdsweb.u-strasbg.fr/cgi-bin/qcat?J/A+A/435/459

were available. For the V_h prediction we also used a multiparametric relation including such galaxy characteristics as total magnitude, surface brightness index, morphological type and the red to blue diameter ratio. We selected the galaxies with $V_{pred} \leq 9500\,km\,s^{-1}$. We augmented our target list with galaxies with optically measured radial velocities but without HI line-widths.

Altogether, we incuded in the target list 340 flat galaxies. Among them, 268 objects have been observed so far, and 121 galaxies have been detected in HI. The observations were performed in the total power mode (ON-OFF) combining a reference field 5 min earlier in RA with respect to the on-source position. The telescope half power beam width at 21 cm wavelength is 9′.3. The dual polarization receiver had a system temperature of 30 K. The 1024 channel autocorrelator was split into 4 banks of 256 channels each, shifted in frequency by 11 MHz with respect to each other in order to cover a total velocity range from 250 km s^{-1} to 9050 km s^{-1} using a bandwidth of 12.5 MHz per bank. The resulting channel spacing was 10.4 km s^{-1}. For galaxies with known radial velocity we used a bandwidth of 6.25 MHz per bank yielding a channel spacing of 5.2 km s^{-1}. In this case no frequency offsets between different banks were applied. For the majority of the objects we have to apply Hanning smoothing (or some equivalent) to improve the signal-to-noise ratio.

3. Results

HI profiles of the observed galaxies are presented in Fig. 1 in order of increasing RA starting in the bottom left corner. Optical and measured HI parameters are given in Table 1. Its columns contain: (1) the RFGC number; (2, 3) equatorial coordinates for the epoch J2000.0 in the format hhmmss.s, ddmmss; (4, 5) blue major and minor angular diameters corresponding approximately to the $25^m/\square''$ isophote, in arcmin; (6) integrated blue magnitude; (7) Galactic extinction in the *B* band, according to Schlegel et al. (1998); (8) morphological Hubble type where Sb = 3, Sc = 5, Sd = 7; (9) index of the mean surface brightness (1 – high, 2 – low, 3 – very low, 4 – extremely low) (Karachentsev et al. 1999a); (10) the measured HI flux, in Jy km s^{-1}; (11) the peak level of the emission line and its rms noise, in mJy; (12) the mean heliocentric radial velocity and its error, in km s^{-1}; (13–15) the line widths at the 50%, 25%, and 20% level of the peak emission, in km s^{-1}. Errors of velocity measurements depend on the velocity resolution, the signal-to-noise ratio and the shape of the line profiles. The half power line width is given for all detected galaxies. Line widths at lower levels are only given when the signal-to-noise ratio allows the measurement. The symbol "*" corresponds to a weak line, and the symbol ":" means uncertain estimate. Some additional notes are given at the end of Table 1.

In Table 2 we present optical data and the r.m.s. noise for non-detected RFGC galaxies (in Col. 9). Columns 1 to 8 are the same as in Table 1.

The HI detection rate for our present observations is rather low, being only 45%, in comparison with the 80% detection rate for the Arecibo sample, which is due to the larger beam (and hence lower beam filling factor) of the 100-m radio telescope. Figure 2 presents the HI detection rate versus different galaxy characteristics: angular diameter, morphological type, and the surface brightness index.

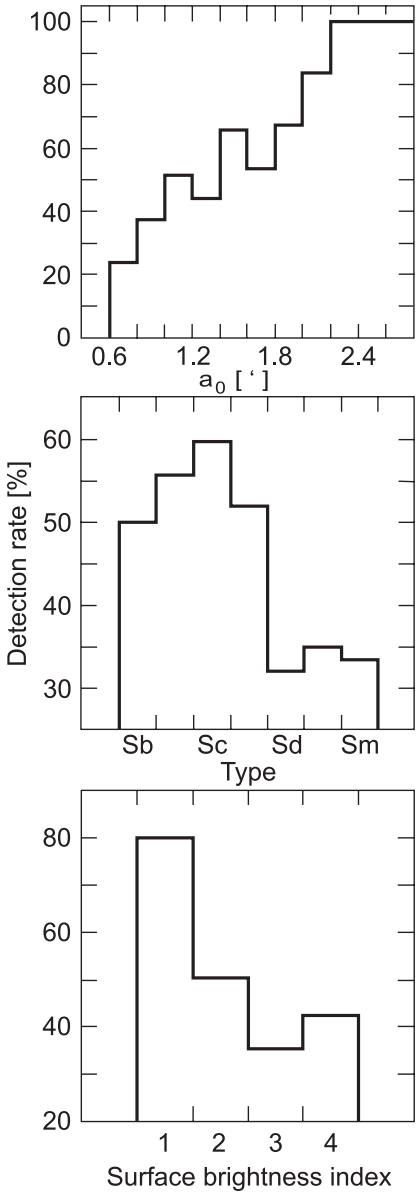

Fig. 2. The HI detection rate (%) versus different galaxy characteristics: angular diameter (*top*), morphological type (*middle*) and surface brightness index (*bottom*).

As expected, the detection rate decreases smoothly with the angular diameter of the galaxies and their mean surface brightness. The fraction of detected galaxies has a tendency to fall from early type objects towards late ones. This might be caused by weak HI emission from smaller distant late-type galaxies (galaxies of type Sd–Sm are generally smaller than galaxies of type Sb–Sc and hence contain less HI (Roberts & Haynes 1994).

Table 3. The distribution parameters for the observed flat galaxies.

Parameter	Mean	St. dev.	Skewness	Kurtosis
$\log(W_{50})$	2.36	0.20	−0.88	1.90
$\log(A_{25})$	1.23	0.24	−0.56	0.33
$\log(L_B)$	10.00	0.60	−0.58	0.28
$\log(M_{\rm HI})$	9.53	0.51	−0.90	1.19
$\log(M_{25})$	10.40	0.57	−0.75	1.05
$\log(M_{\rm HI}/L_B)$	−0.47	0.37	−0.32	0.62
$\log(M_{\rm HI}/A_{25}^2)$	7.07	0.32	0.06	0.94
$\log(M_{25}/L_B)$	0.40	0.24	−0.15	1.54
$\log(M_{25}/M_{\rm HI})$	0.87	0.35	−0.04	0.52
$\log(A_{25} \cdot W_{50})$	3.59	0.39	−0.64	0.68

4. Some global optical and HI characteristics

We calculated global parameters of the galaxies using their radial velocity reduced to the Local Group centroid, $V_{\rm LG}$, as a distance indicator. The apex parameters $\{V_{\rm a} = 316$ km s^{-1}, $l_{\rm a} = 93°$, $b_{\rm a} = -4°\}$ were adopted according to Karachentsev & Makarov (1996). The total "calculated" B magnitude from the RFGC catalog (Karachentsev et al. 1999a) was corrected for Galactic extinction A_B and internal absorption A_i (Verheijen 2001) where

$$A_i = [1.6 + 2.8(\log V_{\rm m} - 2.2)] \log(a_0/b_0), \quad (1)$$

if $V_{\rm m} > 42.7$ km s^{-1}, otherwise $A_i = 0$. For the edge-on[1] galaxies we adopt for the maximum rotational velocity $V_{\rm m} = (W_{50})/2$. The line width was reduced for cosmological broadening and turbulence (Tully & Fouqué 1985). The integrated HI mass was determined as

$$\log(M_{\rm HI}/M_\odot) = \log F + 2\log(V_{\rm LG}/H_0) + 5.37, \quad (2)$$

where F is the 21-cm flux in Jy km s^{-1} and $H_0 = 75$ km s^{-1} Mpc^{-1}. The "total" (indicative) mass of a galaxy was calculated as

$$\log(M_{25}/M_\odot) = 2\log(W_{50}) + \log(a_{\rm c}) + \log(V_{\rm LG}/H_0) + 3.92, \quad (3)$$

where $a_{\rm c}$ is the angular diameter a_0 corrected for Galactic extinction and inclination. After exclusion of 5 "doublets" (see Notes to Table 1) and RFGC 3231 (the case of probable Galactic HI emission), our sample of 120 RFGC galaxies is characterized by the following statistical parameters presented in Table 3.

These data yield a mean mass-to-luminosity value for flat galaxies of 2.5, and a mean hydrogen mass fraction of ~13%, which are typical values for the discs of spiral galaxies. On average, our sample demonstrates about the same mean characteristics but with larger standard deviations as the sample of flat galaxies observed with the Arecibo telescope (Giovanelli et al. 1997) and studied by Karachentsev et al. (1999b). In Table 4 we present the mean values of different parameters and their standard errors separately for each morphological type from Sb to Sm.

The average hydrogen surface brightness, $M_{\rm HI}/A_{25}^2$, does not change significantly along the Hubble sequence, in accordance with previous conclusions reached by Haynes & Giovanelli (1984) for isolated spiral galaxies. The total mass-to-luminosity ratio decreases smoothly from 2.7 for Sbc to 1.6 for Sm types. The fraction of hydrogen mass in the total mass grows from early types towards later ones, as was noted by Roberts & Haynes (1994). The average hydrogen mass-to-luminosity ratio is almost constant (the values for Sb and Sm galaxies are affected by low number statistics).

Table 5 gives the mean global parameters for flat galaxies having different optical surface brightness indices. We see that the data reveal no significant differences in the global characteristics between bright and faint objects.

5. Correlations of global parameters

Table 6 gives numerical parameters of the linear regression $y = kx + c$, where the logarithms of various global characteristics for flat galaxies are used as the variables x and y. We give the correlation coefficient $\rho(x, y)$ and its standard deviation $\sigma(y)$ in Cols. 4 and 5; Cols. 6 and 7 contain the regression parameters k and c and their standard errors.

In Fig. 3 we visualize the "Holmberg relation", optical luminosity L_B versus linear diameter A_{25} (in kpc) corresponding to angular diameter $a_{\rm c}$. The present sample of flat galaxies is given by open squares, while a comparison sample, the nearby galaxies within 10 Mpc (Karachentsev et al. 2004), is given by filled circles. The agreement for the relation between luminosity and linear diameter for both samples is excellent. For $A_{25} \geq 2.5$ kpc and $\log L_B \geq 8$ both samples overlap. The local sample extends to low values in luminosity and optical diameter, one reason for the increasing noise in the relation; some of the local galaxies are situated in the *zone of avoidance* which yields large errors in diameter and luminosity. From Table 6 we see that there are good correlations between global parameters like linear diameter A_{25}(kpc), luminosity L_B in solar units, the total HI mass $M_{\rm HI}$ and the total mass M_{25} both in solar units. For example we show the correlation between the mass of neutral hydrogen $\log M_{\rm HI}$ and the linear diameter $\log A_{25}$ in Fig. 4 and between total mass M_{25} and optical luminosity $\log L_B$ in Fig. 5. In both cases we give the present sample (open squares) and a comparison sample, the nearby galaxies within 10 Mpc (as filled circles).

In rows 6–12 of Table 6 the relations between different variables and the HI line width, which is independent of galaxy distance, are presented. The relation between $\log(A_{25})$ and $\log(W_{50})$ is rather weak. The values of $\log(M_{25}/L_B)$ and $\log(W_{50})$ are weakly correlated contrary to the data for the Arecibo flat galaxy sample. Note also a certain relation between the HI mass and the galaxy "angular momentum". For our sample, $\log(M_{\rm HI}) = 1.07\log(A_{25} \cdot W_{50}) + 5.69$, being in fact the same as for the flat Arecibo galaxy sample, $\log(M_{\rm HI}) = 1.08\log(A_{25} \cdot W_{50}) + 5.60$ (Karachentsev et al. 1999b).

[1] By definition RFGC galaxies have axial ratios $a/b \geq 7$, i.e. edge-on assuming an intrinsic axial ratio of 0.2. For an intrinsic axial ratio of 0.1 the correction of the line width to edge-on would be at most 0.5%.

Table 4. Average values of different parameters versus morphological types for the flat galaxy sample.

N	Type	$\log(M_{\rm HI}/A_{25}^2)$	$\log(M_{25}/L_B)$	$\log(M_{25}/M_{\rm HI})$	$\log(M_{\rm HI}/L_B)$
5	Sb	6.55 ± 0.18	0.23 ± 0.07	1.26 ± 0.14	−1.03 ± 0.16
15	Sbc	7.00 ± 0.08	0.43 ± 0.06	0.97 ± 0.09	−0.53 ± 0.08
31	Sc	7.06 ± 0.05	0.41 ± 0.03	0.90 ± 0.05	−0.49 ± 0.06
27	Scd	7.18 ± 0.07	0.42 ± 0.05	0.82 ± 0.06	−0.40 ± 0.08
23	Sd	7.08 ± 0.05	0.41 ± 0.04	0.84 ± 0.08	−0.44 ± 0.07
14	Sdm	7.10 ± 0.09	0.38 ± 0.08	0.82 ± 0.09	−0.44 ± 0.10
4	Sm	7.10 ± 0.11	0.21 ± 0.17	0.30 ± 0.15	−0.09 ± 0.08

Table 5. Average values of different parameters versus the surface brightness index.

N	SB	$\log(M_{\rm HI}/A_{25}^2)$	$\log(M_{25}/L_B)$	$\log(M_{25}/M_{\rm HI})$
5	1	7.29 ± 0.11	0.32 ± 0.10	0.64 ± 0.15
15	2	7.07 ± 0.04	0.41 ± 0.03	0.86 ± 0.04
31	3	7.02 ± 0.06	0.38 ± 0.04	0.91 ± 0.06
27	4	7.06 ± 0.12	0.37 ± 0.13	0.93 ± 0.17

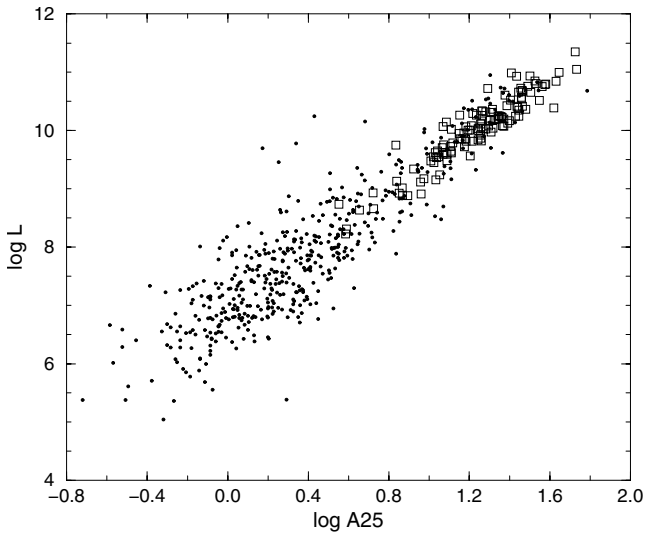

Fig. 3. Blue optical luminosity L_B versus linear diameter A_{25} for the present sample of flat galaxies (open squares) and a comparison sample of nearby galaxies within 10 Mpc (filled circles).

In summary, the correlations between global parameters for our sample are quantitatively the same as for the Arecibo sample of flat galaxies and also for the nearby galaxy sample.

6. Conclusion

We present HI observations made with the Effelsberg 100-m radio telescope of 268 edge-on spiral galaxies from the Revised Flat Galaxy Catalogue (Karachentsev et al. 1999a). Fluxes, radial velocities and line widths are given for 121 detected galaxies, as well as upper limits for 147 nondetected ones. The rate of detection is 45%, increasing from small to large galaxy angular diameter, from late to early morphological type, and from low to high surface brightness.

The average global optical and HI properties of galaxies in our sample agree well within the observational errors with the results of flat galaxies observed by Giovanelli et al. (1997) with the Arecibo telescope. There are strong correlations between global parameters like linear diameter A_{25}, luminosity L_B, the

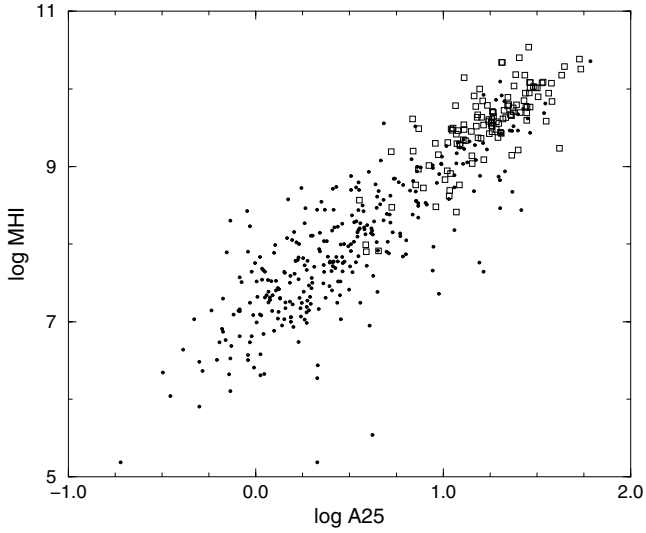

Fig. 4. HI mass $M_{\rm HI}$ versus linear diameter A_{25} for the present sample of flat galaxies (open squares) and a comparison sample of nearby galaxies within 10 Mpc (filled circles).

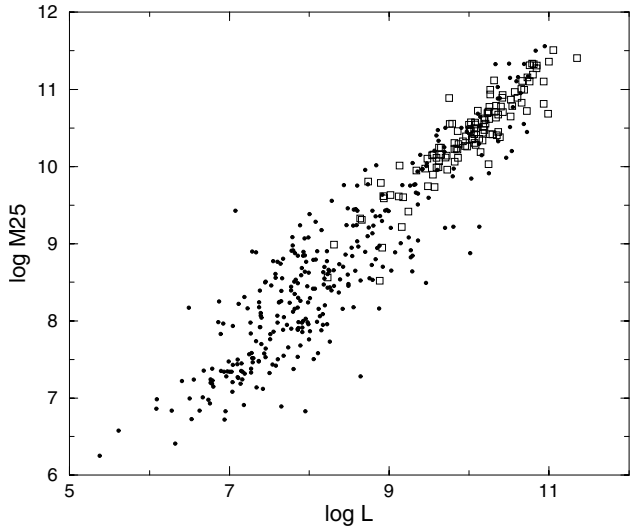

Fig. 5. Total mass M_{25} versus blue optical luminosity L_B for the present sample of flat galaxies (open squares) and a comparison sample of nearby galaxies within 10 Mpc (filled circles).

Table 6. Parameters of the linear regression $y = kx + c$ for the global characteristics of the flat galaxies.

N	y	x	$\rho(xy)$	$\sigma(y)$	$k \pm \sigma_k$	$c \pm \sigma_c$
1	$\log(M_{HI})$	$\log(A_{25})$	0.79	0.32	1.67 ± 0.12	7.48 ± 0.15
2	$\log(M_{25})$	$\log(A_{25})$	0.82	0.33	1.95 ± 0.13	7.99 ± 0.16
3	$\log(L)$	$\log(A_{25})$	0.94	0.21	2.37 ± 0.08	7.09 ± 0.10
4	$\log(M_{HI})$	$\log(L)$	0.79	0.31	0.67 ± 0.05	2.86 ± 0.47
5	$\log(M_{25})$	$\log(L)$	0.92	0.22	0.87 ± 0.03	1.73 ± 0.34
6	$\log(A_{25})$	$\log(W_{50})$	0.57	0.20	0.69 ± 0.09	-0.39 ± 0.21
7	$\log(M_{25}/L)$	$\log(W_{50})$	0.33	0.23	0.40 ± 0.10	-0.54 ± 0.25
8	$\log(M_{HI}/L)$	$\log(W_{50})$	−0.33	0.35	-0.60 ± 0.16	0.95 ± 0.38
9	$\log(M_{25}/M_{HI})$	$\log(W_{50})$	0.56	0.29	1.00 ± 0.13	-1.49 ± 0.32
10	$\log(M_{HI}/A_{25}^2)$	$\log(W_{50})$	0.19	0.32	0.31 ± 0.15	6.34 ± 0.35
11	$\log(M_{HI})$	$\log(A_{25} \cdot W_{50})$	0.82	0.29	1.07 ± 0.07	5.69 ± 0.25
12	$\log(M_{HI})$	$\log(W_{50})$	0.66	0.38	1.69 ± 0.18	5.56 ± 0.42

total HI mass M_{HI} and the total mass M_{25} as expected for spiral galaxies.

The total mass-to-luminosity ratio and HI mass-to-total mass ratio change along the Hubble sequence. Average global parameters such as HI surface density and total mass-to-luminosity ratio are practically independent of the optical surface brightness of flat galaxies and of their linear diameter. The mean total mass-to-luminosity ratio for the sample galaxies is about 2.5 in solar units. There seems to be a tight linear correlation between the hydrogen mass and the angular momentum of flat galaxies.

Acknowledgements. This work is based on observations with the 100-m radio telescope of the MPIfR (Max-Planck-Institut für Radioastronomie) at Effelsberg. This research was supported by RFFI-DFG grant 02-02-04012. We thank the anonymous referee for many useful comments.

References

Giovanelli, R., Avera, E., & Karachentsev, I. D. 1997, AJ, 114, 122
Haynes, M. P., & Giovanelli, R. 1984, AJ, 89, 758
Karachentsev, I. D. 1989, AJ, 97, 1566
Karachentsev, I. D., & Makarov, D. I. 1996, AJ, 111, 535
Karachentsev, I. D., Karachentseva, V. E., & Parnovskii, S. L. 1993, AN, 314, 97 (FGC)
Karachentsev, I. D., Karachentseva, V. E., Kudrya, Yu. N., et al. 1999a, Bull. SAO, 47, 5 (RFGC)
Karachentsev, I. D., Karachentseva, V. E., & Kudrya, Yu. N. 1999b, Pis'ma Astron. Zh., 25, 3
Karachentsev, I. D., Karachentseva, V.E., Kudrya, Yu. N., et al. 2000a, Astron. Zh., 77, 175
Karachentsev, I. D., Karachentseva, V. E., Kudrya, Yu. N., et al. 2000b, Bull. SAO, 50, 5
Karachentsev, I. D., Karachentseva, V. E., Huchtmeier, W. K., & Makarov, D. I. 2004, AJ, 127, 2031
Karachentseva, V. E., & Karachentsev, I. D. 1998, A&AS, 127, 409
Kudrya, Yu. N., Karachentsev, I. D., Karachentsev, I. D., et al. 2003, A&A, 407, 889
Makarov, D. I., Burenkov, A. N., & Tyurina, N. V. 2001, Astron. Lett., 27, 213
Roberts, M. S., & Haynes, M. P. 1994, ARA&A, 32, 115
Schlegel, D. J., Finkbeiner, D. P., & Davis, M. 1998, ApJ, 500, 525
Skrutzkie, M. F., Schneider, S. E., Stiening, R., et al. 1997, in The Impact of Large Scale Near-IR Sky Surveys, ed. F. Garzon, et al. (Dordrecht: Kluwer), ASSL, 210, 25
Tully, R. B., & Fouqué, P. 1985, ApJS, 58, 67
Verheijen, M. A. 2001, ApJ, 563, 694

Online Material

Article published by EDP Sciences and available at http://www.edpsciences.org/aa or http://dx.doi.org/10.1051/0004-6361:20041394

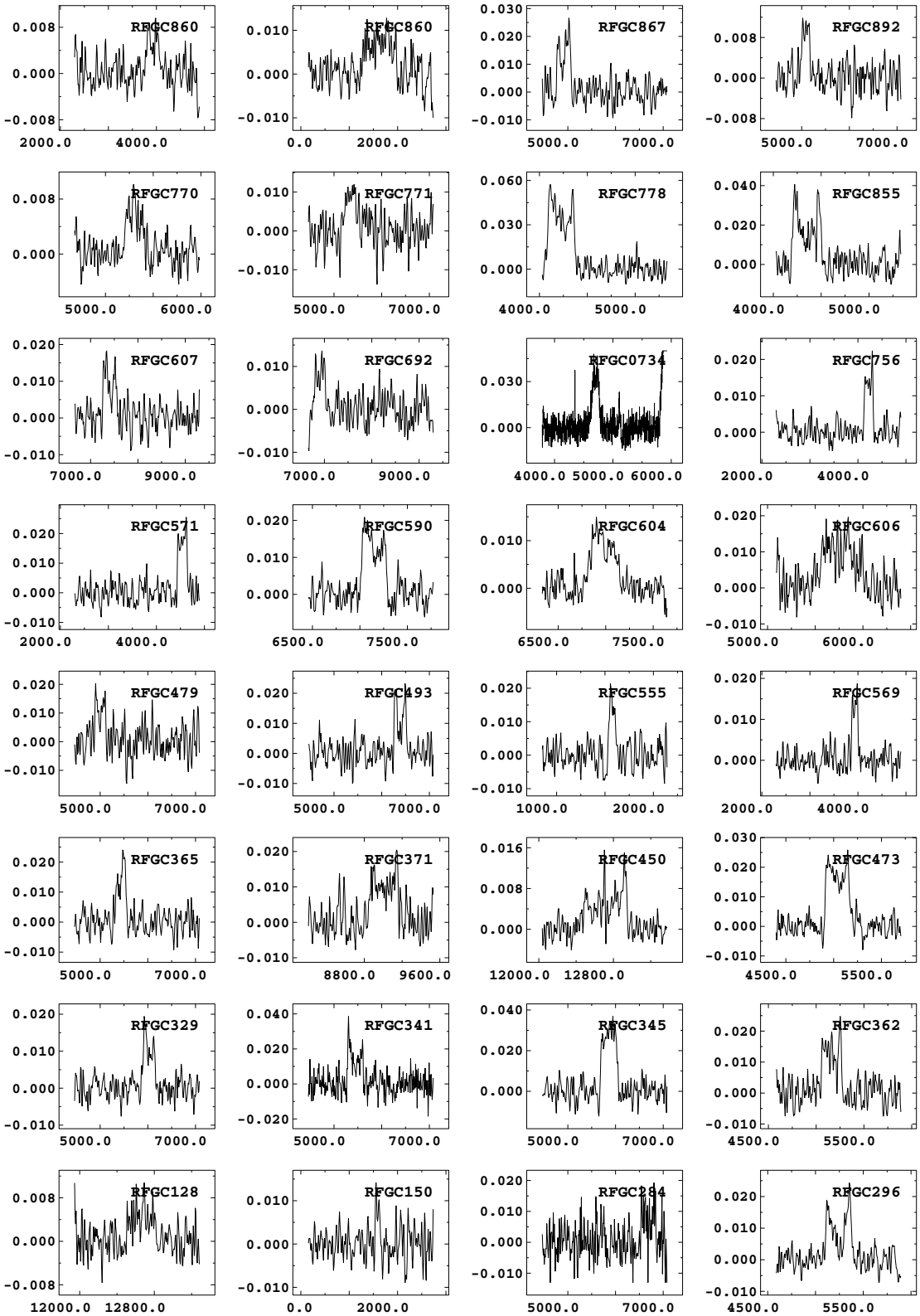

Fig. 1. HI profiles for 121 RFGC galaxies (from Table 1) in ascending order of RA starting at the bottom left corner.

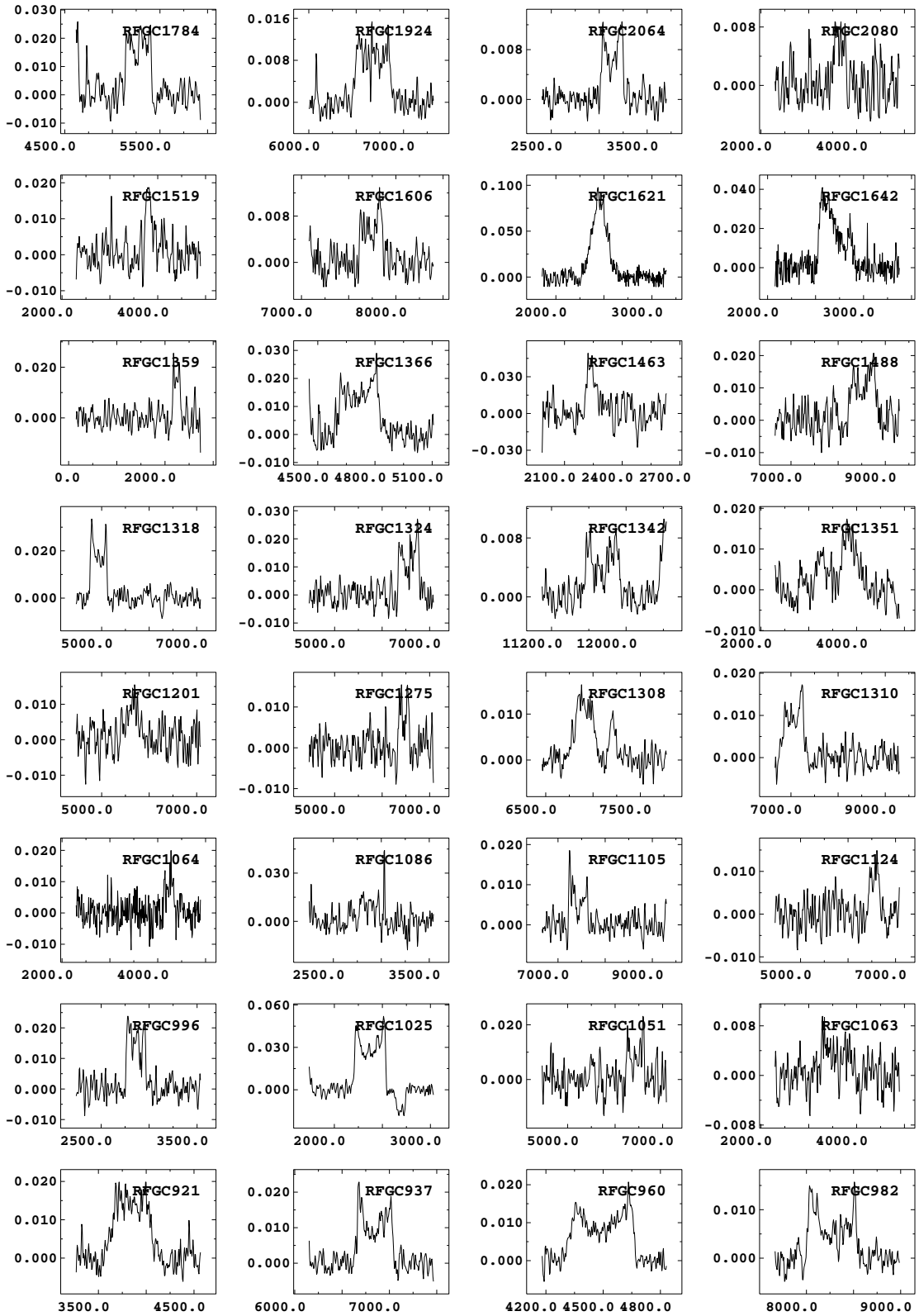

Fig. 1. continued.

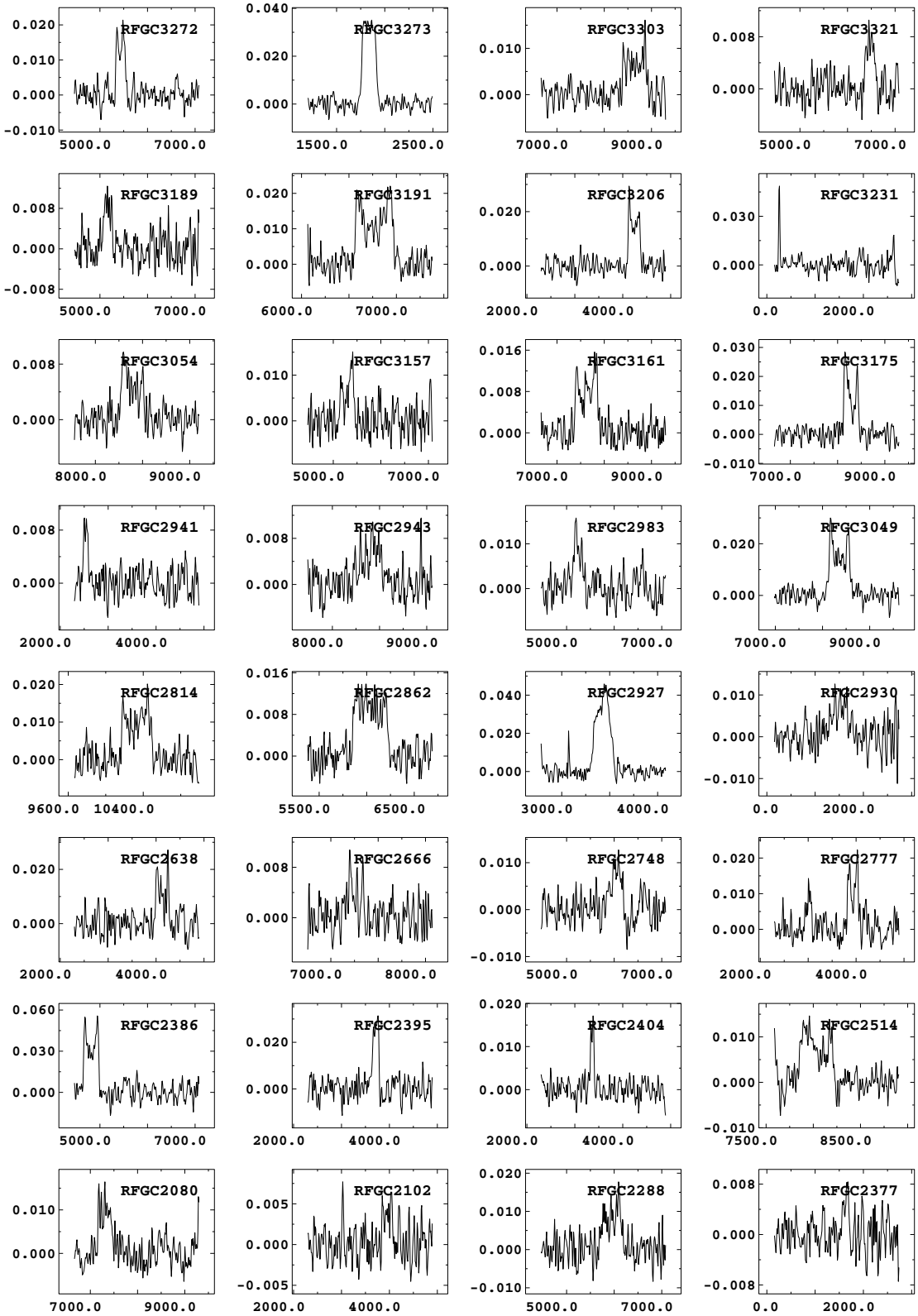

Fig. 1. continued.

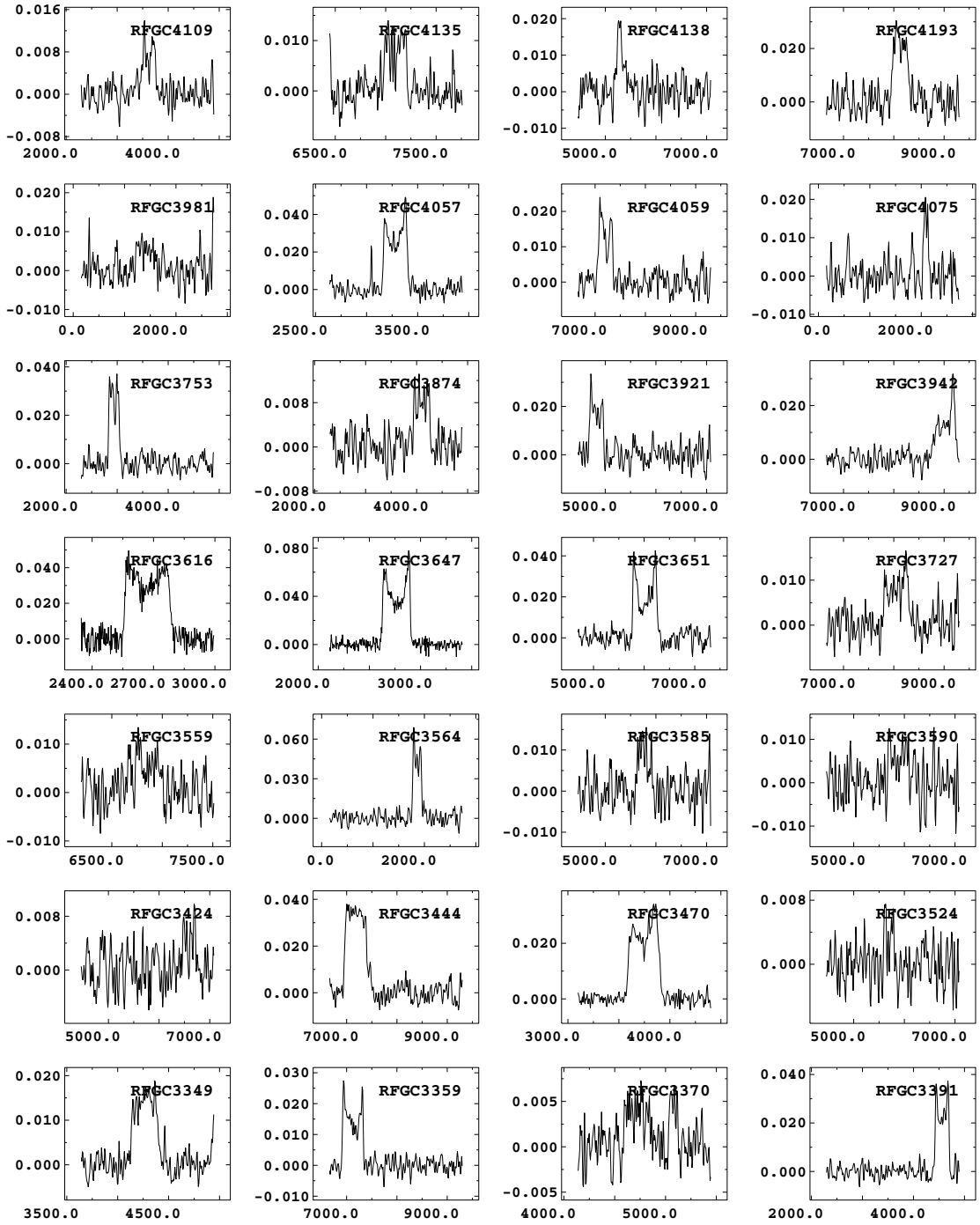

Fig. 1. continued.